

Binary collision dynamics of fuel droplets

N. Ashgriz and P. Givi

An experimental study has been carried out in which the collision dynamics of two *n*-hexane fuel droplets are studied. The experiments are performed on the collision of two burning droplets, as well as two nonburning droplets, to assess the influence of the high temperature combustion environment on the dynamics of the collision.

The results indicate that as the Weber number is increased, the collision type moves toward higher energy collision, and for the same Weber number, different types of collisions, depending on the local value of the collision impact parameter, may occur. In the range of the Weber numbers studied, the results show that for the nonburning droplets, the collision type can be bouncing, grazing, temporary coalescence-satellite generating, or permanent coalescence, depending on the local value of the impact parameter. For the burning droplets in the same initial Weber number range, only temporary coalescence and permanent coalescence are observed.

Keywords: droplet collision; spray combustion; evaporating droplets

Introduction

Sprays are used in many combustion devices such as jet propulsion engines, diesel engines, industrial boilers, and furnaces. These sprays consist of droplets containing a wide range of sizes and velocities. The details of the combustion process are intimately affected by the spatial and temporal distributions of liquid and vaporized fuel within the combustion chamber, which in turn, depend on the details of the initial atomization process itself.

Based on the experimental observations, sprays are generally divided into three regions¹ as shown in Figure 1: dilute spray region, dense spray region, and churning flow region. In the churning flow region, a liquid jet emerging from the nozzle deforms and breaks into small droplets. In the dense spray region, droplets are very closely spaced so that there is a strong direct droplet-to-droplet interaction. The number density of the droplets in this region is so high that it is not possible to do any kind of accurate measurement using available instrumentations. In the dilute spray region, on the other hand, droplets are spaced far enough from one another so that direct interaction between them is usually negligible. In this region, well-known empirical correlations for isolated drops can be used to calculate the exchange rates of mass, momentum, and energy between an individual drop and the surrounding gas.¹

Most of the spray combustion models used today are well developed for the predictions of dilute sprays. The initial spray characteristics (droplet size distribution, velocity distribution, and trajectories), however, must be input into these models. These characteristics are usually obtained from cold, noncombusting spray measurements. Since the combustion environment can greatly alter the initial spray characteristics, significant uncertainty in the input parameters to these dilute spray models exists. Therefore, a spray model that couples the dilute spray region directly to the nozzle exit, that is, a model that considers the churning flow and dense spray regions, is superior in that the initial conditions are the well-defined nozzle exit conditions.

Recent advancements in the modeling aspects of sprays have resulted in the developments of new mathematical models for the prediction of aerodynamic atomization of liquid jets.² The numerical results obtained by applying these models, however, are usually in poor agreements when compared with experimental data in the initial region of the spray. For instance,

the numerical results of Martinelli *et al.*³ predict a mean droplet diameter much smaller than those measured experimentally by Hiroyasu and Kadota.⁴

Hiroyasu and Kadota have obtained droplet size distributions in diesel fuel sprays under conditions approximating those in an engine cylinder. The measurements are performed just downstream of the nozzle, where the spray is dilute enough so that measurements are possible. Their droplet size distribution measurements from an ensemble of more than 3000 drops show that the Sauter mean diameter for a spray produced from single-hole nozzle at back pressure of 1.1 Mpa is about 42 μm . Whereas, the numerical results of Martinelli *et al.*³ based on a modified aerodynamic theory predict a mean drop diameter of only 6 μm under similar conditions. Martinelli *et al.* indicate that the main reason for the discrepancy between the numerical predictions and the experimental measurements of the droplet size is due to the droplet coalescence in the dense region of the spray. They mention that the experimental data of Hiroyasu and Kadota are collected at the downstream of the dense spray region, whereas the theory predicts the droplet sizes in a domain just upstream of this region (Figure 1). The droplet collision process that may occur in this dense spray region can cause an increase in the droplet size farther downstream of the spray. Therefore, to correctly predict the spray behavior, accurate models of droplet collision are required.

Statistical models developed by Martinelli *et al.*³ (based on the earlier work of O'Rourke and Bracco⁵) to represent the influence of the droplet collisions predict a correct overall

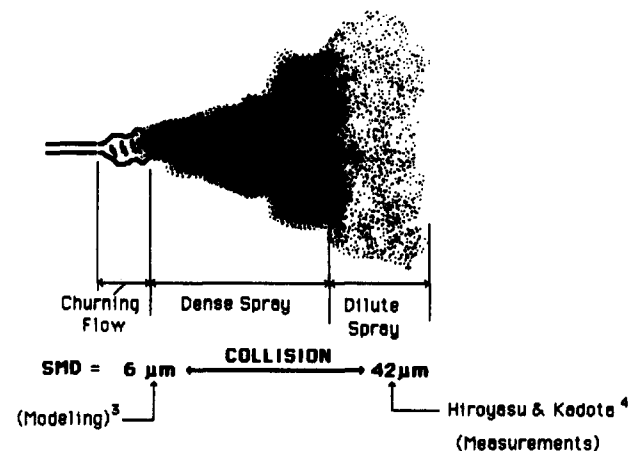


Figure 1 Three regions of a liquid spray

Department of Mechanical and Aerospace Engineering, State University of New York, Buffalo, NY 14260, USA

Received 28 September 1986 and accepted for publication 8 February 1987

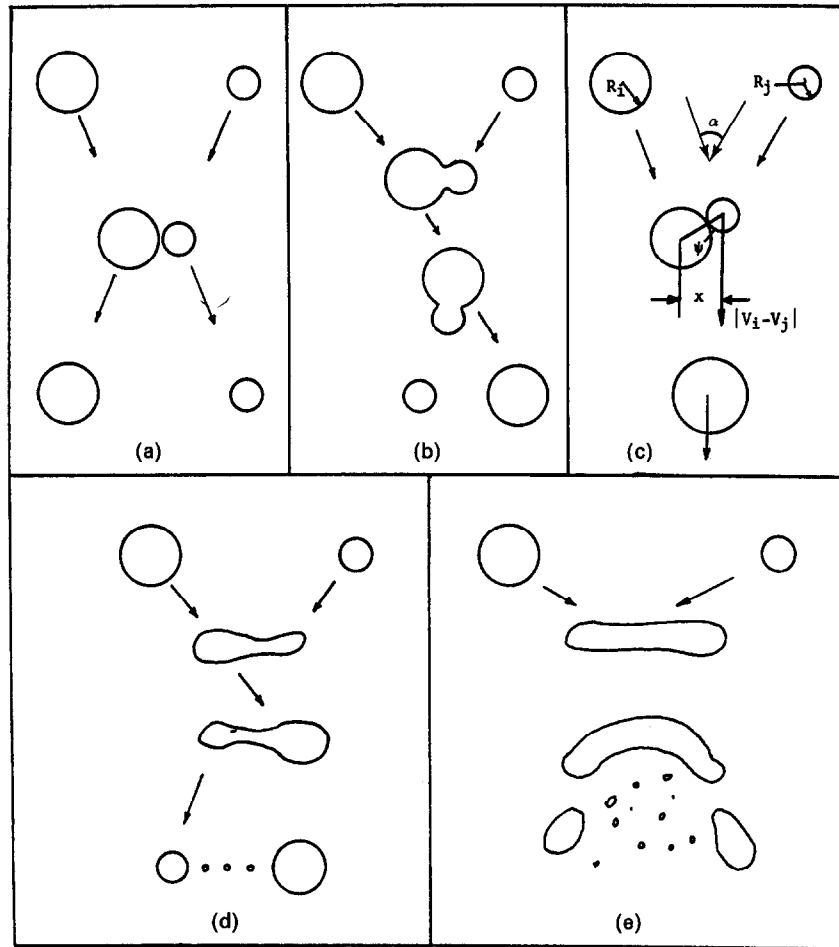


Figure 2 Types of collision

behavior of sprays. Many of the assumptions made in these models, however, require further investigations, namely, the different mechanism of droplet collision and coalescence and the effects of environmental conditions on the outcome of these collisions.

Most of the experimental studies on the collision dynamics of interacting droplets have been reported by investigators in the atmospheric sciences^{6,7} and the thermophysics of the wet steam turbines.^{8,9} These studies have been mainly encouraged by the lack of knowledge about the exact growth mechanism of water drops. The interactions observed for two water drops can be categorized into five different types, as shown in Figure 2:

(1) Bouncing collision—the contact of the surfaces are prevented by the intervening air film resulting in bouncing of the droplets after the collision (Figure 2a).

(2) Grazing collision—the droplets just touch one another slightly without coalescence (Figure 2b).

(3) Permanent coalescence collision—the droplets coalesce and remain united permanently (Figure 2c).

(4) Temporary coalescence—satellite generating collision—the droplets coalesce temporarily with a subsequent separation accompanied by satellite drops (Figure 2d).

(5) Shattering collision—with very high energy collision, shattering occurs in which numerous tiny droplets are expelled radially from the periphery of the interacting drops (Figure 2e).

The type of droplet interactions observed for two colliding water droplets depends on the drop sizes and velocities and the existing dynamic forces between the droplets, as well as other

Notation

D Droplet diameter

Lp_i Laplace number = $\frac{D_i \rho \sigma}{\eta^2}$

R Droplet radius

V Droplet velocity

We_{ij} Weber number = $\frac{|V_i - V_j|^2 \rho D_j}{\sigma}$

X Impact parameter

α Angle between the trajectories of two droplets at the time of collision (trajectory angle)

Δ Droplet diameter ratio = $\frac{D_i}{D_j}$

ψ Collision angle

ρ Liquid droplet density

σ Surface tension

η Liquid droplet viscosity

Subscripts

cr Critical

i Larger droplet

j Smaller droplet

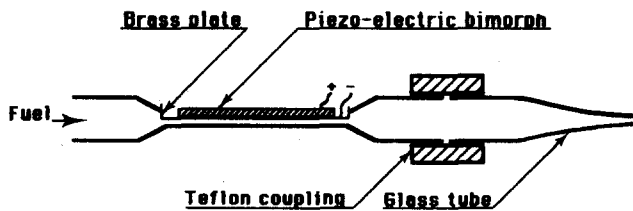


Figure 3 Droplet generator

parameters. There has been some work to determine the boundaries between the regions of hydrodynamic conditions under which various types of interaction may take place.⁶⁻¹⁰ For example, Adam *et al.*⁶ indicate that for the interaction of two similar water drops with diameters of $D = 60 \mu\text{m}$ and relative velocities, $|V_i - V_j|$, less than a critical velocity of 2.2 m/s, all collisions result in coalescence, whereas for relative velocities greater than the critical velocity, fragments are formed. For particles with $D = 5 \mu\text{m}$, the magnitude of the critical velocity increases up to 9.4 m/s. Arkhipov¹¹ attempted to describe such behavior by carrying out a cinematographic investigation of two colliding water droplets with different sizes and velocities. His experiments for droplets with diameter size ratios in the range of $1.1 < D_i/D_j < 2.7$ and a Laplace number of about $L_p = 10^5$ indicate that the different mechanisms of droplet interaction is independent of both the droplets diameter ratio and the collision angle ψ (ψ is the angle formed by the line connecting the centers of the droplets at the moment of contact and the vector of their relative velocity, as shown in Figure 2c) and is dependent on only the magnitude of the Weber number. Arkhipov observed that for Weber numbers less than 2.0, droplets bounce; for Weber numbers in the range of 2–15, coalescence occurs; for Weber numbers in the range of 15–50, coalescence takes place with a consequent separation; and for Weber numbers greater than 50, fragments form.

The conclusions of Arkhipov,¹¹ however, do not completely agree with the results of Brazier-Smith *et al.*¹² The latter's experiments on two colliding water droplets in a diameter range of 150 to 750 μm and an absolute velocity difference ($|V_i - V_j|$) in the range of 0.3 to 3.0 m/s show the Weber number alone cannot characterize the process of droplet collision and there is a critical collision angle (ψ_{cr}), above which the droplets separate after the collision and below which they stay coalesced. They estimated an equation for this critical angle by comparing the kinetic energy of rotation of the droplet formed by the coalescence and the difference between the surface energies of this drop and the original droplets before the collision.

The results of these meteorological studies on water droplet collision is encouraging in establishing the criteria for the mechanism of rain drop growth. These results, however, are not completely applicable to typical sprays, since there are still no concrete conclusions on the effect of all the important nondimensionalized parameters characterizing the dynamics of collision. These results, also, are not completely valid for describing the collision dynamics of typical hydrocarbon fuels under the influence of combustion.

It would be useful to study the effects of all the important parameters such as the Weber number, droplet Reynolds number, droplet size, droplet velocity, velocity ratios, impact parameter, and Damkohler number (in the case of combustion) on the dynamics of droplet collisions. These studies, however, would require highly detailed experimental efforts. In this paper, we examine only the isolated effects of the Weber number and the global influence of the combustion. Moreover, the values of the Weber numbers and the impact parameters are kept in a range where only the dynamics of the bouncing, grazing, temporary coalescence, and permanent coalescence collisions can be assessed; the study of the mechanism of the shattering collision is left for future efforts.

For the present tasks, an experimental effort is undertaken. In this experiment, two streams of uniform size droplets are aimed

at each other at different collision angles while other parameters are kept constant. The collision angle is changed so that the effect of the collision energy on the collision mechanism can be studied systematically. The initial Weber number is kept approximately in the range of 2–15, which has been reported to be the region for the coalescence type collision for water drops.¹¹ To assess the influence of the high temperature environment on the dynamics of collision, both burning and nonburning droplets are considered. A simple configuration like this is an excellent system in which to study the mechanism of droplet diameter increase due to collision and the effects of high temperature environment on the dynamics of the collision.

Experimental setup

An experimental setup is designed and developed to produce streams of liquid droplets with uniform sizes.¹³ The advantage of using streams of droplets, instead of two single droplets, is that it is unnecessary to synchronize the collision of two streams. Each stream is independent of the other, and the droplet size and trajectory of each stream can be varied independently.

A uniform stream of droplets can be produced by the vibration of a piezoelectric crystal epoxied to the body of an ejector tube (see Figure 3). Since the contraction and expansion of the piezoelectrical crystal under electric pulse is very small, a bilaminar plate arrangement is used. This plate arrangement is constructed by flattening a small length of a 13 mm diameter copper tube and then cutting and replacing this flattened section by a thin sheet of brass. A piezoelectric bimorph is then epoxied on the brass piece. When the axially polarized piezoelectric plate is exposed to an electric field (using a function generator) in the direction of the polarization, an axial expansion and a radial contraction of the piezoelectric plate appear. The axial expansion is small, and the radial contraction generates a concentric moment that bends the composite plate (the piezoelectric bimorph and the brass plate) toward the fuel chamber resulting in a pressure impulse.

The droplet size is controlled by the orifice diameter of a glass nozzle that is attached to the exit of each ejector tube. Glass nozzles are made simply by heating and pulling a glass tube and sanding the pulled end to make different orifice sizes.

Figure 4 shows a schematic of the experimental setup. Each droplet generator has its own fuel pumping system and is connected to a function generator and an oscilloscope. The fuel is pumped by a pressurized nitrogen tank to keep a constant fuel flow rate without any fluctuations. Fuel flow rates through each

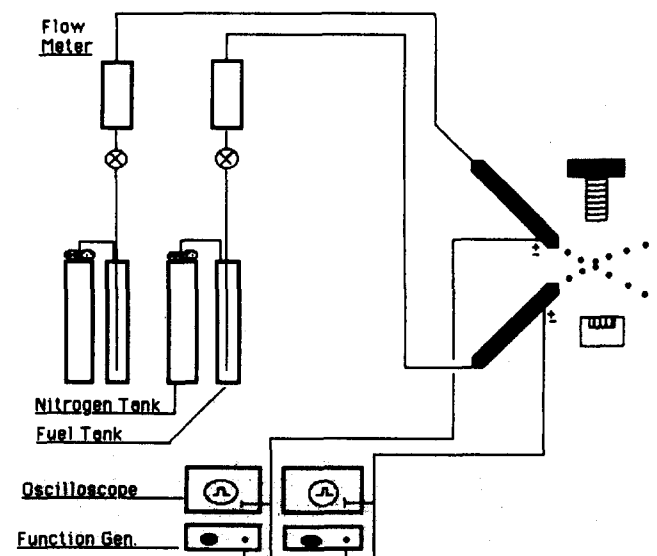


Figure 4 Experimental setup

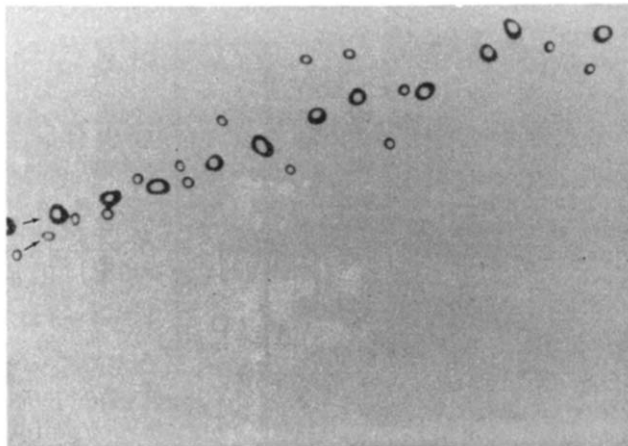


Figure 5 Collision of two streams of droplets with trajectory angle = 15° at nonburning condition

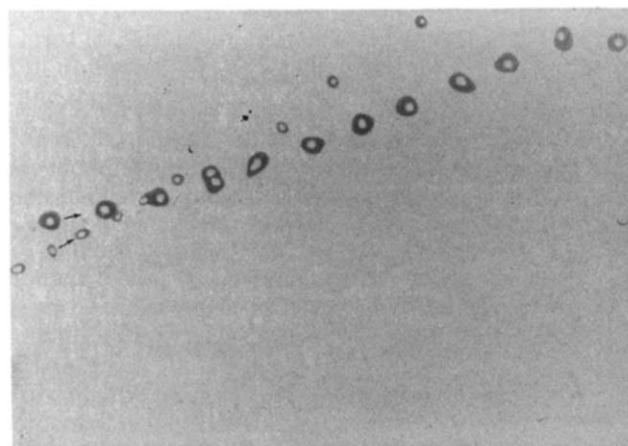


Figure 6 Collision of two streams of droplets with trajectory angle = 15° at burning condition

nozzle are measured by conventional rotameters. Both ejector tubes are connected to special stands so that their trajectories can be easily changed. A 35 mm camera with a bellows and macro-lens is focused at the collision point of the two droplets, and the collision mechanism of the two droplets is captured on the film using single flash illumination. The droplet size and droplet trajectories are obtained from these magnified pictures.

Presentation of results

Experiments are performed to study the dynamics of collision of two streams of *n*-hexane droplets, one with a diameter of $800\ \mu\text{m}$ and speed of $90\ \text{cm/s}$ and the other with a diameter of $440\ \mu\text{m}$ and speed of $120\ \text{cm/s}$. The droplet size and droplet speed in each stream are kept constant while the trajectories of the two streams are changed to vary the trajectory angle α (shown in Figure 2). The free flight distance of the droplets before collision is short enough so that the droplet trajectory and velocity do not change significantly. Varying the trajectory angle changes the collision energy by changing the relative velocity between the droplets. Collision of both nonburning and burning droplets is observed. In the nonburning experiments, the collision process occurs at room temperature, whereas in the burning experiments, both streams are ignited, and the collision process takes place under combusting conditions. Although extensive experimental observations were made, for this paper, only those results related to droplet coalescence are presented. First the results of our experimental observations are given and then the analysis of these observations is presented.

Observations

Typical pictures of the process of droplet collision are shown in Figures 5–10. Figure 5 shows the collision of two droplets at a trajectory angle of $\alpha = 15^\circ$ under nonburning conditions. At this angle, it is observed that the droplets either bounce after the collision (bouncing collision) or touch one another slightly without coalescence (grazing collision).

Figure 6 shows the influence of the combustion on the droplet collision at the same trajectory angle ($\alpha = 15^\circ$). In this case, it is observed that all the collisions result in permanent coalescence. The main reason for the different collision dynamics observed between this case and the nonburning case (Figure 5) is due to the effects of temperature increase from chemical reactions. Increasing the droplet's temperature results both in the direct reduction of the surface tension of the droplets in both streams and in indirect reductions of the surface tension due to creation of the fuel vapor in the interface of the droplets. These reductions of the surface tension would allow the droplets to penetrate one another at a lower collision energy and remain in contact for a longer time. Increasing the trajectory angle α to 22° influences the collision dynamics of the droplets under nonburning conditions, as shown in Figure 7. In this case, droplets either coalesce permanently or graze one another (grazing collision). The differences between the process of collision in this case ($\alpha = 22^\circ$) and the previous case ($\alpha = 15^\circ$) are due to the higher collision energy of the larger trajectory angle. As we will show, this energy has a direct influence on the mechanism of the collision, and an increase in the magnitude of

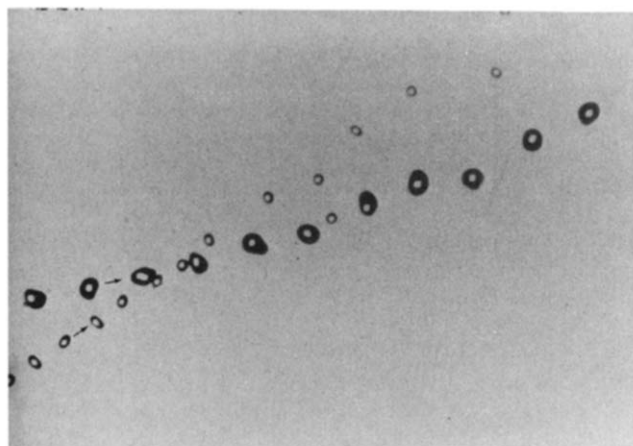


Figure 7 Collision of two streams of droplets with trajectory angle = 22° at nonburning condition

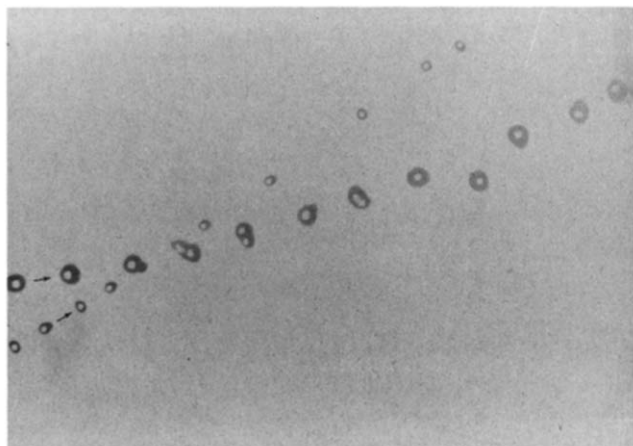


Figure 8 Collision of two streams of droplets with trajectory angle = 22° at burning condition

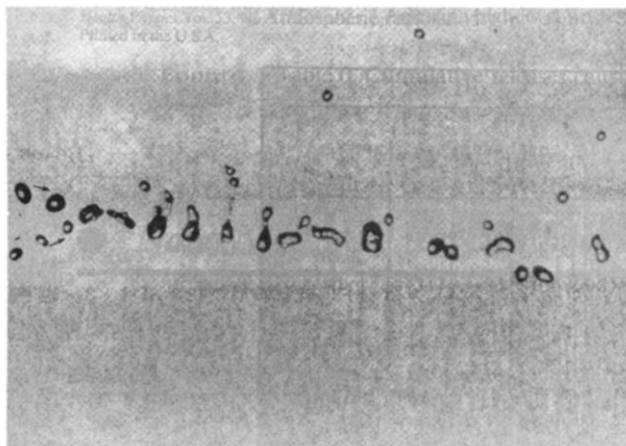


Figure 9 Collision of two streams of droplets with trajectory angle = 45° at nonburning condition

this energy results in an increase in the observed number of coalescing droplets.

Figure 8 shows the effects of burning of the droplets on the process of collision at this angle. Comparing Figure 8 with Figure 7 indicates that, under burning conditions, there are no observed grazing collisions, and all the collisions of the droplets result in permanent coalescence. Again, this is due to the reduction of the surface tension as discussed for the $\alpha = 15^\circ$ case. Comparing Figure 8 with Figure 6 indicates that, under burning conditions, the increase in the trajectory angle (α) from 15 to 22 does not appreciably influence the collision dynamics of the droplets.

Figure 9 shows the process of collision for a trajectory angle of 45° for nonburning droplets, and Figure 10 shows this for burning droplets. These two figures indicate that, at this trajectory angle, the droplets after collision coalesce either permanently (permanent coalescence) or temporarily with consequent separation (temporary coalescence). Comparing Figures 9 and 10 with Figures 7 and 8 indicates that increasing the trajectory angle from 22° to 45° has a reverse effect on the increase of the total number of permanent coalescences after the collision. This is because, at this trajectory angle, the magnitude of the surface tension energy of the resulting single coalesced droplet is not large enough to prevent the consequent breakup of this droplet into two drops in the trajectory of the initial "mother" droplets before the onset of collision. Finally, comparing Figure 10 with Figure 9 indicates that, at the trajectory angle of 45°, combustion does not seem to influence the collision process significantly, except that under burning conditions, a larger number of observed colliding droplets separate after the collision.

Analysis

Our observations indicate that for different values of the trajectory angle (α), different types of collision may occur and that for the same angle (α), two types of collisions may result. This is due to the variation of the collision angle ψ ¹² or, more clearly, to the variations of the impact parameter X ($X = (R_i + R_j \sin \psi)$). For collision to occur, X must lie in the range between zero and $(R_i + R_j)$. The experimental results indicate that, for each droplet collision trajectory of α , there may exist a critical impact parameter, X_{cr} , that the collision type will change, and its value must be determined to characterize the collision type.

Direct measurement of the parameter X or ψ requires high resolution three-dimensional photography (for example, laser holography) and has not been performed in this experiment. Instead, whenever possible, the critical values of the parameter

are estimated by the equation suggested by Brazier-Smith *et al.*¹²

$$\psi_{cr} = \arcsin \left[\frac{f(D_i/D_j)}{We_{ij}} \right]^{1/2} \quad (1)$$

where

$$f = \frac{4.8[1 + (D_i/D_j)^2 - [1 + (D_i/D_j)^3]^{2/3}][1 + (D_i/D_j)^3]^{11/3}}{(D_i/D_j)^6[1 + (D_i/D_j)]^2} \quad (2)$$

In this study, $D_i/D_j = 1.8$, which results in $f = 13$. Therefore, Equation 1 will be valid only for $We > 13$. The only Weber number in this study lying above 13 is $We = 14$ for the collision of 45° trajectory angle. For $We = 14$, the critical collision angle is $\psi = 76^\circ$, and the impact parameter is $X = 600 \mu\text{m}$. The critical parameters for the nonburning condition could not be calculated using Equations 1 and 2; thus no numeric value is specified for them. For the burning condition, only one type of collision is observed, except for $We = 14$. Therefore, the critical parameter is just $X = R_i + R_j$, which indicates that if the droplets collide only one collision type will be observed. Thus, for this study $X_{cr} = R_i + R_j = 620 \mu\text{m}$. To characterize the collision dynamics observed in our experiments, the influence of the Weber number is examined, and the results of our analysis are compared with the results of Arkhipov¹¹ for colliding water droplets in the same Weber number range.

In calculating the Weber number for the nonburning droplet collision, the surface tension value at 25°C was used; however, for the burning case, the value at 60°C was used, which is approximately equal to the wet-bulb temperature of the *n*-hexane fuel.

Table 1 compares our results with Arkhipov's results. Table 1 indicates that for Weber numbers less than 2 and $X < X_{cr}$, the collision of the fuel droplets is bouncing type, which is in good agreement with Arkhipov's results. However, in our experiments, grazing collisions are also observed for Weber numbers in the same range and $X > X_{cr}$. For Weber numbers in the range of 2–14, our results indicate that the collision might be either permanent coalescence, temporary coalescence, or grazing collision, depending on the value of the collision angle. The results of Arkhipov in the same Weber number range, however, predict only coalescence type collision, not the other types of collisions observed in our experiments. As our experiments indicate, the impact parameter can have a significant influence on the outcome of the collision, especially for colliding fuel droplets under nonburning conditions. Therefore, any model constructed to describe the droplet collision must explicitly include the effect of the impact parameter (or the collision angle) in the formulations.

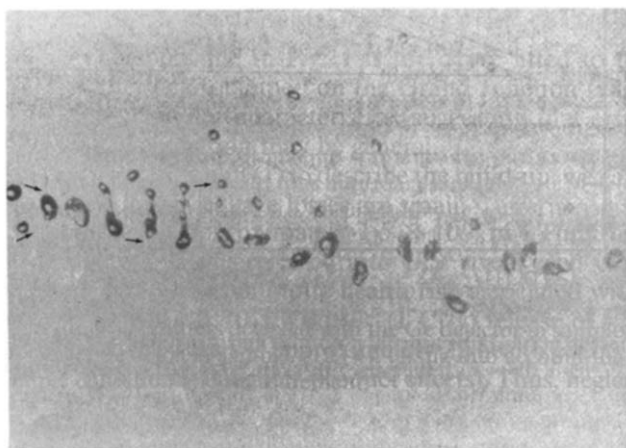


Figure 10 Collision of two streams of droplets with trajectory angle = 45° at burning condition

Table 1 Summary of results

Case	Condition	We	α	X_{cr}	ψ	$X < X_{cr}$	$X > X_{cr}$
1	Cold	2	15	—	—	Grazing collision	Bouncing
2	Burning	2.5	15	620	90	Coalescence	Coalescence
3	Cold	3.5	22	—	—	Coalescence	Grazing collision
4	Burning	4.2	22	620	90	Coalescence	Coalescence
5	Cold	7	35	—	—	Coalescence	Grazing collision
6	Burning	9	35	620	90	Coalescence	Coalescence
7	Cold	11	45	—	—	Temporary coalescence	Coalescence
8	Burning	14	45	600	76	Temporary coalescence	Coalescence

Conclusion

These experimental results show that the Weber number and the collision impact parameter have a significant effect on the dynamics of the collision of fuel droplets. The results further indicate that the chemical reactions can also have a direct influence on the outcome of these collisions.

The photographic study of two *n*-hexane fuel droplets with Weber numbers in the range of 2–14 indicates that, as the Weber number is increased, the collision type moves toward higher energy collision and, for the same Weber number, different types of collisions, depending on the value of the collision impact parameter (or the collision angle), may occur.

The outcome of the collision of two nonburning droplets is compared with the outcomes of two burning droplets under similar initial conditions (the same initial droplet diameters, velocities, and trajectory angle). The results indicate that, for nonburning droplets, the collision type can be bouncing, grazing, temporary coalescence, or permanent coalescence, depending on the local value of the impact parameter. For burning droplets with the same initial condition, however, only temporary coalescence and permanent coalescence are observed. This difference is due to the influence of the high temperature environment (from combustion) in increasing the Weber number of colliding droplets, shifting the collision type toward a higher energy collision mechanism. Therefore, it is indicated that any mathematical model attempting to describe the dynamics of droplet collisions in burning conditions must explicitly include the effects of temperature in the formulation.

We are now extending our studies to investigate the influence of other important parameters, such as the Reynolds number, velocity ratio, and diameter ratio, on the dynamics of the colliding droplets. A wider range of Weber numbers is also being studied to assess the effects of chemical reaction on the types of collisions not investigated in this paper.

References

- 1 Faeth, G. M. Evaporation and combustion of sprays. *Prog. Energy Comb. Sci.*, 1983, **9**, 1–76.
- 2 Reitz, R. D. Atomization and other breakup regimes of a liquid jet. PhD thesis, Princeton University, 1978, 1375-T.
- 3 Martinelli, L., Bracco, F. B., and Reitz, R. D. Comparisons of computed and measured dense spray jets. *AIAA Progress in Astronautics and Aeronautics*, 1984, 95.
- 4 Hiroyasu, H., and Kadota, T. Fuel droplet size distribution in diesel combustion chamber. *SAE*, paper no. 740715, 1974.
- 5 O'Rourke, P. J., and Bracco, F. V. Modelling of drop interactions in thick sprays and a comparison with experiments. *Stratified Charged Auto Eng. Conf., Inst. Mech. Eng.*, 1980, pub. ISBN 0-85298-4693, 101–116.
- 6 Adam, J. R., Lindbland, N. R., and Hendricks, C. D. The collision coalescence and disruption of water drops. *J. Appl. Phys.*, 1968, **39**, 5173–5180.
- 7 Gunn, R. Collision characteristics of freely falling water drops. *Science*, 1965, **150**, 695–701.
- 8 Ryley, D. J., and Bennett-Cowell, B. N. The collision behavior of steam-borne water drops. *Int. J. Mech. Sci.*, 1967, **9**, 817–833.
- 9 Ryley, D. J., and Wood, M. R. Thermodynamics and Fluid Mechanics Group Convention. *I. Mech. E.*, paper 1, Liverpool, 1966.
- 10 Ashgriz, N. Observation of the collision of two non-burning and burning mono-dispersed droplet streams. Presented at the Technical Meeting of the Combustion Institute, Philadelphia, Pennsylvania, Nov. 1985.
- 11 Arkhipov, V. A. *et al.* Experimental study of drops interaction at collisions. *J. Appl. Mech. Tech. Phys. U.S.S.R.*, 1978, **2**, 73–77, referenced in Podvysotsky, A. M. and Shraiber, A. A. Coalescence and break-up of drops two-phase flows. *Int. J. Multiphase Flow*, 1984, **10**(2), 195–209.
- 12 Brazier-Smith, P. R., Jennings, S. G., and Latham, J. The interaction of falling water drops: coalescence. *Proc. Roy. Soc. Lond.*, 1972, **A326**, 393–408.
- 13 Ashgriz, N., and Yao, S. C. Development of multi-orifice impulsed spray generator for heterogeneous combustion experiments. *ASME/JSME Thermal Eng. Conf. Proc.*, 1984, **2**, 433–439.